Transgenic TDP-43 and endogenous TDP-1 Caenorhabditis elegans ALS models show motor deficits and age-dependent neurodegeneration

J. Alex Parker (ja.parker@umontreal.ca)
Université de Montréal
Sarah Duhaime
Université de Montréal
Constantin Bretonneau
Université de Montréal

Article

Keywords:

Posted Date: April 20th, 2022

DOI: https://doi.org/10.21203/rs.3.rs-1555653/v1

Additional Declarations: No competing interests reported.

Abstract

Amyotrophic lateral sclerosis (ALS) is a fatal neurodegenerative disease characterized by a progressive and selective loss of motor neurons. ALS is incurable and there are no effective treatments available for people living with the disease. About 90% of the cases are sporadic whereas 10% are familial, and patients usually die two to five years after symptom onset. Many genes are associated with ALS, including mutations in the gene encoding TDP-43. We developed a transgenic *Caenorhabditis elegans* model expressing human mutant TDP-43(Q331K) in GABAergic motor neurons. We also obtained by mutagenesis and CRISPR-Cas9 gene-editing physiologically accurate models based on mutations in *tdp-1*, the *C. elegans* orthologue of *TARDBP*. Our results show that both transgenic TDP-43 and endogenous TDP-1 models recapitulate key aspects of ALS such as motor deficits and age-dependent neurodegeneration causing paralysis. However, only the TDP-43 mutation had a negative effect on lifespan. These models provide different physiological expression of mutant proteins and thus phenotypes of varying intensity levels. They will be useful tools to elucidate new pathogenic mechanisms of ALS as well as being suitable for drug discovery and therapeutic development.

Introduction

Amyotrophic lateral sclerosis (ALS) is a neurodegenerative disease linked to aging, as are Alzheimer's, Parkinson's and Huntington diseases (Gitler, Dhillon et al. 2017). ALS is a fatal disease characterized by a progressive and selective loss of upper and lower motor neurons. Patients with ALS usually die from respiratory failure 2 to 5 years after the onset of symptoms (Tao and Wu 2017, Oskarsson, Gendron et al. 2018). This disease appears late in age and usually affects individuals between 40 and 60 years old with an average of 55 years (Taylor, Brown et al. 2016).

About 90% of the cases are sporadic and 10% are familial (Zarei, Carr et al. 2015). More than 200,000 people are currently living worldwide with ALS with an incidence rate between 0.6 and 3.8 per 100,000 person-year according to recent studies (Arthur, Calvo et al. 2016, Longinetti and Fang 2019). Unfortunately, ALS is incurable and there are no effective treatments available for people living with the disease. Indeed, no treatment has made it possible to significantly slow or stop the progression of the disease. Despite many clinical trials, the only drugs approved by the US FDA are Riluzole and Radicava (Edaravone) (Cruz 2018). Both of these drugs are meant to slow the progression of the disease and extend the life expectancy of patients (Abe, Itoyama et al. 2014). The glutamatergic neurotransmission inhibitor, Riluzole, has a modest effect on survival (average extended lifespan of 2–3 months) whereas the antioxidant drug, Edaravone, appears to be effective in slowing the progression of ALS in the early stages of the disease (Jaiswal 2019). However, recent population studies have shown that Riluzole may help prolong survival from 6 to 19 months compared to the previous clinical trials (Andrews, Jackson et al. 2020).

In the past few decades, research has made it possible to associate several genetic abnormalities to ALS but the most common are the following. Mutations in the *C9orf72* gene represent the largest proportion

(30–40%) of patients with familial ALS (Balendra and Isaacs 2018, Shi, Lin et al. 2018). Mutations in the *SOD1* (superoxide dismutase 1) gene represent around 15–20% of the cases and mutations in the *FUS* (Fused in Sarcoma) oncogene account for approximately 5% of familial ALS cases (Blair, Williams et al. 2010, Moller, Bauer et al. 2017, Pansarasa, Bordoni et al. 2018). Finally, about 5% of the cases have mutations in the *TAR DNA Binding Protein-43* (*TARDBP*) gene, which codes for the TDP-43 protein (Valdmanis, Daoud et al. 2009, Mejzini, Flynn et al. 2019).

TDP-43 (TAR DNA binding protein-43) is a RNA/DNA binding protein with a molecular weight of 43 kDa. This protein is highly conserved, expressed ubiquitously and is part of the large hnRNP family (heterogeneous nuclear ribonucleoprotein) (Van Deerlin, Leverenz et al. 2008). This family includes proteins which can bind to RNA in a sequence-specific manner with the presence of RRMs (RNA recognition motifs). TDP-43 contains 414 amino acids (aa) and its coding gene, *TARDBP*, is located on chromosome 1. This protein includes an N-terminal region (1-102 aa) with a nuclear localization signal (NLS, 82–98 aa), two RRMs: RRM1 (104–176 aa) and RRM2 (192–262 aa), a nuclear export signal (NES, 239–250 aa), and a C-terminal region (274–414 aa) which contains a domain rich in glutamine and asparagine (345–366 aa), and a glycine-rich region (366–414 aa) (Fig. 1A). The C-terminal region seems to be particularly involved in the pathology of TDP-43 in ALS. As a prion-like domain, this region is disorganized and predisposed to pathological aggregation (Dhakal, Wyant et al. 2020). Also, the majority of mutations and phosphorylation sites associated with ALS are located in this C-terminal region (Prasad, Bharathi et al. 2019).

TDP-43 is mainly located in the nucleus where it performs its main functions, but it can also shuttle to the cytoplasm to play other roles. This protein has many functions including being involved in transcription, splicing, translation as well as stabilization, maturation and transport of mRNA (Prasad, Bharathi et al. 2019). TDP-43 binds to approximately 6,000 mRNA transcripts, representing almost 30% of the entire transcriptome (Polymenidou, Lagier-Tourenne et al. 2012).

During stress, TDP-43 assembles into stress granules (SG) in the cytoplasm, and is involved in the assembly and maintenance of the integrity of these structures (Hergesheimer, Chami et al. 2019). In pathological conditions like ALS, the cytoplasmic concentration of TDP-43 increases, and the protein is hyperphosphorylated, ubiquitinated and cleaved which leads to the formation of inclusion bodies (Scotter, Chen et al. 2015). These inclusions can be particularly damaging for cells such as motor neurons (Prasad, Bharathi et al. 2019).

Years of research have made it possible to learn more about ALS and different factors implicated. However, despite the advancement of knowledge on this proteinopathy, ALS remains complex and multifactorial, making the causes of this disease still largely unknown. To be able to study the molecular mechanisms, the signaling pathways involved in ALS and possibly develop effective treatments, the development of research models is essential.

To do so, we turned to the model organism *Caernorhabditis elegans*. This nematode has several advantages including a small size (1 mm at adulthood), a compact genome, hermaphroditic-self

reproduction, rapid development cycle (3 to 5 days at 20°C), simple genetic manipulation, a well-studied simple nervous system as well as constant transparency during its short lifespan (3–4 weeks) (Sulston and Horvitz 1977, Johnson and Wood 1982, Altun and Hall 2009). Depending on the bioinformatics approach used, between 60–80% of human genes have an ortholog in *C. elegans* (Kaletta and Hengartner 2006, Shaye and Greenwald 2011). Thus, the conservation of genes, molecules and genetic interactions in this model is a clear advantage for studying genetics. Additionally, the *C. elegans* genome contains an orthologue of *TARDBP*, named *tdp-1*. The resulting TDP-1 protein has 414 amino acids (isoform c), 38% of homology and conserved domains with the human protein except it lacks the glycine-rich domain (Fig. 1C). TDP-1 is primarily nuclear but can shuttle to the cytoplasm, is expressed in most tissues and has conserved functions. Like TDP-43, TDP-1 exhibits RNA binding activity and plays a role in the regulation of protein homeostasis (Zhang, Hwang et al. 2012). TDP-1 also plays a role in adult lifespan, hyperosmotic response, response to oxidative stress and several other processes (Vaccaro, Tauffenberger et al. 2012).

We wanted to develop a *C. elegans* model reflecting an identical mutation found in patients and subsequent mouse models to aid translational studies (Arnold, Ling et al. 2013, White, Kim et al. 2018). We generated transgenic *Caenorhabditis elegans* models expressing human wild-type TDP-43(WT) and mutant TDP-43(Q331K) in GABAergic motor neurons (Fig. 1AB). The human Q331K mutation is located in the glycine-rich domain, where the majority of mutations are found in ALS patients (Prasad, Bharathi et al. 2019).

We also obtained by mutagenesis and CRISPR-Cas9 a physiologically accurate model based on the mutation R393C in *tdp-1* (Fig. 1D). This endogenous mutation is located in the equivalent *C. elegans* domain, the C-terminal domain. Our objective was to characterize these models and determine if they can recapitulate key aspects of ALS disease such as motor deficits and age-dependent neurodegeneration causing paralysis. We believe that the TDP-1 model may reflect more precisely the physiological expression of the gene in the human disease because of its mutation in an endogenous gene and in the absence of potential artefacts resulting from overexpression. To do so, we explored the impact of these TDP-43/TDP-1 mutations on the physiological aspects of the models and assessed the repercussions of these genetic defects on the integrity of the motor nervous system.

Results

Following plasmid integration into the *C. elegans* genome, the relative expression levels of *TARDBP* mRNAs were measured in the TDP-43-Q331K-WT transgenic models by RT-qPCR to confirm the transgenes are indeed expressed. The endogenous *unc-47* gene was used for normalization since the transgene was expressed only in GABAergic motor neurons. The *unc-47* gene encodes a GABA transmembrane transporter in GABAergic motor neurons in *C. elegans* (McIntire, Reimer et al. 1997). The *TARDBP* expression level normalized to *unc-47* of the TDP-43(WT) model is approximately 24.8 times higher compared to the wild type negative control (WT). As for the mutant TDP-43(Q331K), *TARDBP*

expression levels normalized by *unc-47* is approximately 88 times higher than the WT control and approximately 3.5 times higher than TDP-43(WT) (Fig. 1E).

Although the TDP-1(R393C) model is not transgenic and contains a mutation in an endogenous gene, we investigated if the mutation had an impact on the expression of *tdp-1*. *tdp-1* mRNA expression levels normalized to the endogenous *ama-1* gene were also measured in this model by RT-qPCR. The *ama-1* gene encodes a *C. elegans* RNA polymerase II subunit ubiquitously expressed (Rogalski and Riddle 1988). *tdp-1* mRNA expression levels normalized by *ama-1* of mutant TDP-1(R393C) were not significantly different than wild-type *tdp-1* controls, suggesting that the mutation does not affect gene expression (Fig. 1F).

Physiological aspects of the TDP-43 and TDP-1 models

As mentioned earlier, since ALS is an age-related neurodegenerative disease, the life expectancy of affected patients is reduced. The aim of this experiment is to observe whether mutations in TDP-43 and TDP-1 reduce *C. elegans* lifespan. Transgenic mutant TDP-43(Q331K) had a significantly reduced life expectancy compared to WT control, but not with TDP-43 (WT). The WT and TDP-43 (WT) controls had a non-significantly different survival percentage (Fig. 1G). The lifespan of endogenous TDP-1(R393C) mutants did not appear to be reduced compared to the WT control (Fig. 1H). Thereby, only transgenic TDP-43 worms had reduced lifespan, mainly at the beginning of adulthood.

Next, we examined for motility defects using an automated video-microscopy combined with WormLab software approach. Mutant TDP-43(Q331K) crawling speed (µm/s) was significantly reduced at day 1 and 5 of adulthood compared to TDP-43(WT) and WT controls, and all strains crawling speed were similar at day 9 of adulthood (Fig. 2A). Mutant TDP-43(Q331K) swimming speed (µm/s) was significantly lower at days 1, 5 and 9 of adulthood compared to the TDP-43 (WT) and WT controls (Fig. 2B). TDP-43(Q331K) swimming speed tended to remain the same through the days tested. The swimming activity (μm^2/min) corresponds to the surface (μm^2) covered by nematodes during one minute of swimming. Mutant TDP-43(Q331K) swimming activity was significantly lower than the activity of TDP-43 (WT) and WT controls at days 1, 5 and 9 of adulthood (Fig. 2C). TDP-43(Q331K) swimming activity levels also appeared constant through the days tested. Finally, the wave initiation rate (min^{-1}) corresponds to the number of body waves initiated by the head or tail per minute of swimming. Mutant TDP-43(Q331K) wave initiation rate was significantly lower at days 1, 5 and 9 of adulthood compared to the TDP-43 (WT) and WT controls (Fig. 2D). TDP-43(Q331K) wave initiation rate also appeared to be similar at days 1, 5 and 9. Thus, all of these results suggest that the transgenic mutant TDP-43(Q331K) exhibit motility deficits from day 1 of adulthood and these locomotion problems persist through day 9.

Mutant TDP-1(R393C) crawling speed (µm/s) was significantly different from the WT control at day 1 and 5 of adulthood and this decrease in speed was progressive. By day 9 of adulthood, all crawling speeds stabilized. Mutant crTDP-1(R393C) is a positive control to ensure the absence of background mutations in the mutant obtained by mutagenesis. crTDP-1(R393C) crawling speed was not significantly

different from the endogenous mutant at day 5 and 9 of adulthood. crTDP-1 (R393C) crawling speed seemed to be slower at day 1 (Fig. 3A). Mutant TDP-1(R393C) swimming speed (µm/s) was significantly reduced at day 5 and 9 of adulthood compared to the WT control, but not at day 1. crTDP-1(R393C) swimming speed was significantly different from the endogenous mutant at day 1, slightly different at day 5 and not different at day 9 of adulthood (Fig. 3B). Mutant TDP-1(R393C) swimming activity was significantly lower than the activity of WT control at day 5 and 9 of adulthood. crTDP-1(R393C) swimming activity was significantly lower than the endogenous mutant at day 1, but was very similar at day 5 and 9 of adulthood (Fig. 3C). Mutant TDP-1(R393C) wave initiation rate was slightly lower at day 5 compared to the WT control, but not at day 1 and 9 of adulthood. crTDP-1(R393C) wave initiation rate was significantly different from the endogenous mutant at day 1, 5 and 9 of adulthood (Fig. 3D). Thus, according to several WormLab software parameters, the endogenous mutant TDP-1(R393C) has a motility phenotype and this phenotype develops gradually with the age of the nematodes.

Integrity of the motor nervous system

ALS is a neurodegenerative disease that results in the progressive and selective loss of upper and lower motor neurons in humans. The next step in the characterization of the transgenic and endogenous models of *C. elegans* was to assess whether these models exhibit premature neurodegeneration that could contribute to motility phenotypes. The paralysis assay consists of evaluating the progressive loss of motility of worms every day from day 1 to day 12 of adulthood. Nematodes were scored as paralyzed if they failed to move after being prodded with a worm pick. Mutant TDP-43(Q331K) had a significantly higher rate of paralysis compared to the controls TDP-43 (WT) and WT. Paralysis began to manifest in TDP-43(Q331K) worms around day 5–6 of adulthood. By day 12, approximately 40% of TDP-43(Q331K) worms were paralyzed compared to 17% for TDP-43 (WT) and WT controls. Both controls had a very similar rate of paralysis (Fig. 4A). Thus, these results suggest that the transgenic TDP-43 and endogenous TDP-1 mutant exhibit motor deficits causing an age-related paralysis phenotype.

A more direct way to evaluate the integrity of the motor nervous system is to observe whether there is age-related neurodegeneration in GABAergic motor neurons. To visualize the neurons, the transgenic and endogenous mutants were crossed with reporter strains expressing either GFP or mCherry fluorescent proteins in the GABAergic motor neurons from an *unc-47* promoter. GABAergic motor neurons were observed at day 1, 5 and 9 of adulthood using fluorescence microscopy and neurodegeneration was characterized by breaks or gaps along the axonal projections of GABAergic motor neurons.

TDP-43(Q331K) transgenics had a greater percentage of neurodegeneration than the controls TDP-43(WT) and *unc-47::GFP* (WT) at day 1 and 9 of adulthood (Fig. 4B). The transgenic control strain TDP-43(WT) had a rate of neurodegeneration not significantly different from the control WT at day 1, 5 and 9 of adulthood. At day 1, 25% of TDP-43(Q331K) mutants showed neurodegeneration compared to 10% and 11% for the TDP-43(WT) and WT controls, respectively. By day 5 of adulthood, the percentages of neurodegeneration of the three strains appeared similar. At day 9, the percentage of TDP-43(Q331K) population with neurodegeneration was approximately 31% compared to 13% and 17% for TDP-43(WT)

and WT respectively (Fig. 4C). In order to further characterize the neurodegeneration of the transgenic model TDP-43(Q331K), breaks along axonal projections were classified according to whether they were found on the ventral, dorsal or both cords of the GABAergic motoneurons. For TDP-43(Q331K) transgenics compared to controls, neurodegeneration seemed to be more frequent along the ventral cord of nematodes from day 1 to day 9 of adulthood (Fig. 4D). As the animals age, we observed increased incidences of axonal degeneration along both ventral and dorsal cords. Thus, these results suggest that the mutant TDP-43(Q331K) exhibits age-dependent neurodegeneration and that there is a specificity for the localization of this neurodegeneration on GABAergic motoneurons axons to the ventral cord.

Next, we also evaluated the endogenous mutant's motility. TDP-1(R393C) worms had a significantly higher rate of paralysis than WT controls. Paralysis was first observed in TDP-1(R393C) worms around day 6–7 of adulthood compared to WT. Positive control crTDP-1(R393C) also showed increased paralysis compared to WT controls, but not different from endogenous mutant TDP-1(R393C) animals. On day 12, approximately 35% of TDP-1(R393C) nematodes were paralyzed compared to 28% for crTDP-1(R393C) and 17% for WT (Fig. 5A).

We next examined the integrity of GABAergic motoneurons in TDP-1(R393C) animals at days 1, 5 and 9 of adulthood. Endogenous mutant TDP-1(R393C) showed a significant increase in neurodegeneration compared to *unc-47::mCherry* (WT) controls at day 9 of adulthood (Fig. 5B). We observed a progressive increase in the percentage of neurodegeneration from day 1 to day 9. Indeed, at day 1, 11% of the TDP-1(R393C) mutants showed neurodegeneration compared to 10% for the WT control. By day 5 of adulthood, the percentages of neurodegeneration increased to 19% for TDP-1(R393C) and 13% for the WT control. On day 9, the percentage of TDP-1(R393C) nematode population with neurodegeneration were approximately 35% compared to 16% for WT (Fig. 5C). Still with the aim of further characterizing the endogenous model TDP-1(R393C), neurodegeneration seemed to appear more on the dorsal cord of nematodes from day 1 to day 9 of adulthood for the endogenous mutant and the control (Fig. 5D). Also, the proportion of breaks that were found on both ventral and dorsal cords of the endogenous mutant increased with time. All of these results suggest that the mutant TDP-1(R393C) exhibits age-dependent neurodegeneration and that there is a specificity for the localization of this neurodegeneration on GABAergic motoneurons axons to the dorsal cord.

TDP-43 and TDP-1 models for drug discovery

A potential use of these models is their application for modifier screening, including drug screening and the development of new therapeutic strategies. To validate the potential of these new models, we tested them with drugs already approved by the FDA for ALS, namely Riluzole and Edaravone. To test if these models were amenable to drug testing, we used the paralysis assay as it is a fast and efficient method to assess motor function in the presence of drugs (Patten, Aggad et al. 2017).

The paralysis rate of mutant TDP-43(Q331K) treated with 20 µM of Riluzole was not significantly different from the untreated transgenic mutant controls (20 µM DMSO). In addition, TDP-43(WT) and WT controls treated with Riluzole had a higher paralysis rate than untreated ones (Fig. 6A). Mutant TDP-

1(R393C) as well as WT control treated with 20 µM Riluzole had a significantly higher paralysis rate compared to those untreated (20 µM DMSO) (Fig. 6B). Riluzole did not appear to have a neuroprotective effect on TDP-43(Q331K) and TDP-1(R393C) animals, it even increased paralysis in some cases. The percentage of paralysis of mutant TDP-43(Q331K) treated with 20 µM of Edaravone was significantly reduced from approximately 57–36% at day 12 of adulthood (Fig. 6C). The drug Edaravone does not appear to slow the paralysis rate of TDP-43 (WT) and WT compared to the controls untreated, suggesting there may be specificity to the mutant TDP-43 allele. Mutant TDP-1(R393C) treated with 20 µM Edaravone had a significantly lower paralysis rate compared to the untreated controls, going from a percentage of paralysis of approximately 35–21% at day 12 of adulthood (Fig. 6D). These results suggest that Edaravone has a neuroprotective effect on the transgenic TDP-43(Q331K) and endogenous TDP-1(R393C) mutants.

Non-phenotypic TDP-1(R258C) mutant

To ensure that not all mutations in *tdp-1* result in a motor phenotype or age-dependent neurodegeneration, we also obtained another physiologically representative model of the nematode based on the endogenous mutation R258C in *tdp − 1* (Fig. S1A) (Thompson, Edgley et al. 2013). The R258C mutation is located in the first RNA recognition motif domain (RRM1) in *C. elegans*. This is not the area where the majority of mutations are found, but some ALS patients do have mutations in this area. However, R393C mutation is closer to known patient mutations than R258C (Prasad, Bharathi et al. 2019).

Just like the endogenous mutant TDP-1(R393C), *tdp-1* expression levels normalized to *ama-1* of the mutant TDP-1(R258C) were approximately 1.2 times higher compared to the wild-type negative control (WT) (Fig. S1B). Thus, the level of *tdp-1* mRNA expression in this TDP-1 mutant is not significantly different from wild-type control.

Crawling speed, swimming activity and wave initiation rate were also measured in this mutant at day 1, 5 and 9 of adulthood using the same automated video-microscopy combined with WormLab software approach (Fig. S2A-C). Mutant TDP-1(R258C) crawling speed (µm/s) seemed slightly higher than the WT control at day 9, but was not significantly different from WT at day 1 and 5 of adulthood (Fig. S2A). Mutant TDP-1(R258C) swimming activity was not significantly different from the WT control at day 1, 5 and 9 of adulthood (Fig. S2B). The wave initiation rate (min^{-1}) of mutant TDP-1(R258C) was very similar to the WT control at day 1, 5 and 9 of adulthood (Fig. S2C). Mutant TDP-1(R258C) paralysis rate was not significantly different from the WT and crTDP-1(R258C) controls (Fig. S2D). Positive control crTDP-1(R258C) percentage of paralysis was slightly higher than the WT control. Mutant TDP-1(R258C) life expectancy was not significantly different from WT control (Fig. S2E). All these results suggest that the endogenous mutation R258C in *tdp-1* does not induce a motor phenotype and has no impact on lifespan.

Endogenous mutant TDP-1(R258C) did not have a significantly different percentage of neurodegeneration from the *unc-47::mCherry* (WT) control, except at day 1 of adulthood (Fig. S3AB). For

the endogenous TDP-1(R258C) mutant and control, neurodegeneration due to normal aging also seemed to be more frequent on the dorsal cord of nematodes from day 1 to day 9 of adulthood (Fig. S3C). These results suggest that the mutant TDP-1(R258C) does not appear to exhibit age-dependent neurodegeneration other than normal aging. Moreover, there is a specificity for the localization of this normal aging neurodegeneration on GABAergic motoneurons axons to the dorsal cord.

Discussion

There is little consensus about the molecular mechanisms and signaling pathways contributing to ALS. A better understanding of core mechanisms may foster the development of therapeutic strategies to slow the progression of the disease and in the best case, effectively treat affected patients. Therefore, the development of research models is essential in order to be able to study the intrinsic mechanisms of ALS to aid preclinical and ultimately clinical research.

We developed transgenic models of *C. elegans* overexpressing the human wild-type (WT) and mutant (Q331K) protein TDP-43 under a promoter specific for GABAergic motor neurons, *unc-47* (Mariol, Walter et al. 2013, Noma and Jin 2018). The endogenous *tdp-1* gene was not deleted from these transgenic models since this deletion results in several phenotypes. Indeed, studies have shown that the deletion of *tdp-1* preferentially causes the accumulation of double-stranded RNA which can result in splicing problems (Saldi, Ash et al. 2014). In addition, *tdp-1(ok781)* mutants have a slightly prolonged lifespan and also suppress TDP-43 toxicity (Vaccaro, Tauffenberger et al. 2012). Thus, to ensure that the phenotypes observed during the characterization are due only to the mutation of interest, the expression of endogenous *tdp-1* was left untouched.

A caveat of transgenic models is that phenotypes may in part be artifacts of overexpression (Philip, Escobedo et al. 2019). Furthermore, single cell type specific expression using neuronal promoters does not reflect ubiquitous expression of TDP-43. On the other hand, a transgenic model with a strong phenotype could be a useful tool for drug screening given the short lifespan of worms. However, physiologically faithful models may be the best approach for discovering therapeutics with increased relevance to patients. Thus, we also obtained by mutagenesis a physiologically representative model of the nematode based on an endogenous mutation in *tdp-1*, the ortholog of TARDBP (Thompson, Edgley et al. 2013). To ensure that the observable phenotypes are due to the mutation of interest and not to mutations still present in the background, a positive control obtained by CRISPR-Cas9 was generated and named crTDP-1 (R393C).

TDP-43 and TDP-1 mutations have little or no effect on lifespan

The first objective was to explore the impact of TDP-43/TDP-1 mutations on the physiological aspect of the models.

Since ALS is an age-related neurodegenerative disease and patients' life expectancy is reduced, we tested if the mutations in TDP-43 and TDP-1 also caused a reduction in nematode's lifespan. The transgenic mutant TDP-43(Q331K) had a reduced lifespan compared to the TDP-43(WT) and WT controls (Fig. 1E). This decrease was observe more in the first days of adulthood, mainly between days 6 and 22. This suggests that the Q331K mutation in TDP-43 specifically has an impact on the lifespan of nematodes and potentially on their general health span. The endogenous R393C mutation in TDP-1 does not appear to have an impact on the lifespan of nematodes (Fig. 1F). Given the short lifespan of worms, a highly expressed model may be necessary to visualize a lifespan reduction and a single missense mutation in this gene may not result in a robust phenotype even though it is a more physiologically relevant model. This mutation in *tdp-1*, however, appears to influence the motility and integrity of the nervous system of nematodes.

TDP-43 and TDP-1 models display a motility phenotype

According to several locomotion parameters, TDP-43(Q331K) and TDP-1(R393C) mutants exhibit motility defects (Fig. 2,3). One advantage of automated video-microscopy approaches is the possibility of studying different parameters on each nematode individually over time. Day 1, 5 and 9 of adulthood were chosen to be able to visualize the effect of the mutations over a broad spectrum of nematode lifespan.

Whether it is for the crawling speed, swimming speed, swimming activity or wave initiation rate, the transgenic mutant TDP-43(Q331K) motility was significantly reduced at day 1, 5 and 9 of adulthood compared to TDP-43(WT) and WT controls (Fig. 2). In addition, for each parameter, mutant TDP-43(Q331K) levels remained largely stable and constant from day 1 to day 9 of adulthood. This suggests that the transgenic mutant possesses motility problems from early adulthood and that these persist until day 9.

For the endogenous mutant TDP-1(R393C), crawling speed, swimming speed and activity levels gradually decreased over time (Fig. 3ABC). Indeed, the levels of TDP-1(R393C) were little or no different from the WT control at day 1 and they became significantly lower at day 5 of adulthood. For some parameters such as swimming speed, this significant difference also maintained at day 9, but for others, such as crawling speed and activity, the rates tended to stabilize with the WT control. Thus, these results suggest that the endogenous mutant TDP-1(R393C) possesses motility defects, but they manifest themselves progressively with the age of the nematodes. In comparison, another research group generated by CRISPR-Cas9 a *C. elegans* model expressing mutant TDP-1(R219A) (mutation in the RRM1 domain) and analyzed different locomotion parameters at day 7 of adulthood using WormLab software such as track length, wavelength and amplitude (µm) (Flores, Li et al. 2019). These parameters were significantly reduced at the same levels as a knockout *tdp-1(ok803)* model compared to the wild-type control. Concerning the last parameter, the wave initiation rate (Fig. 3D), it is difficult to extrapolate a conclusion for the mutant TDP-1(R393C). The different rates do not decrease proportionately according to days of adulthood. Thus, not all WormLab software parameters may be relevant in order to characterize a mutant phenotypes. Each parameter or group of parameters can be specific for a *C. elegans* model. The WormLab parameter where the motility phenotype seemed the most pronounced for TDP-43(Q331K) and

TDP-1(R393C) mutants was the swimming speed. In fact, while swimming, nematodes make larger and wider movements compared to crawling (Pierce-Shimomura, Chen et al. 2008). This difference in movement is perceptible by the software and results in a greater phenotype compared to the controls.

TDP-43 and TDP-1 models have motility phenotypes

The second objective was to assess the impact of TDP-43(Q331K) and TDP-1(R393C) mutants on the integrity of the motor nervous system. Paralysis assays were conducted to determine if TDP-43 and TDP-1 mutations resulted in age-dependent paralysis. Mutant TDP-43(Q331K) paralysis rate was significantly higher than the controls TDP-43(WT) and WT (Fig. 4A). Paralysis began to manifest in the transgenic mutant around day 5–6 of adulthood. These results were similar with another transgenic mutant that expresses the mutant protein TDP-43(A315T) also in GABAergic motor neurons (Vaccaro, Tauffenberger et al. 2012). Mutant TDP-1(R393C) also exhibited a percentage of paralysis which was significantly higher than the WT control (Fig. 5A). The TDP-1(R393C) paralysis rate started to be different from the WT control around day 6–7 of adulthood. These results suggest that the TDP-43(Q331K) and TDP-1(R393C) mutants have motor deficits resulting in an age-dependent paralysis phenotype. The paralysis of the endogenous mutant began later than the paralysis of the transgenic mutant. These results are consistent with the motility defects observed using the various parameters of the WormLab software. In addition, motor deficits are detected later on for both models with the paralysis assay compared to WormLab parameters, some of which the phenotypes are visible from day 1 of adulthood. Thus, the software approach seems more precise for the detection of weak phenotypic differences.

TDP-43 and TDP-1 mutants exhibit age-dependent neurodegeneration

To assess directly the integrity of GABAergic motor neurons, the TDP-43 and TDP-1 models were evaluated to see if they show age-dependent neurodegeneration. The percentage of neurodegeneration of TDP-43(Q331K) mutant was significantly higher than the controls at day 1 and 9 of adulthood (Fig. 4BC). These results are consistent to another transgenic ALS model expressing mutant TDP-43(M337V) pan-neuronally where in this model, animals had significant neuronal loss as of day 1 of adulthood (Liachko, McMillan et al. 2013). Neuron-specific mutant TDP-43(A315T) also showed motor neuron degeneration (Vaccaro, Tauffenberger et al. 2012). Moreover, pan-neuronal mutant TDP-43(A315T) also had a higher number of neuronal breaks in GABAergic motor neurons at day 1, 3, 5 and 7 compared to WT control (Wong, Pontifex et al. 2018). Neurodegeneration seemed to be found more on the ventral cord of the transgenic strains TDP-43(WT) and TDP-43(Q331K) (Fig. 4D). These data do not correspond to clinical evidence. Indeed, ALS is considered a distal axonopathy meaning that neurodegeneration begins at the ends of axons of motor neurons, or even at the neuromuscular junction (Moloney, de Winter et al. 2014). Cell bodies of GABAergic motor neurons are found on the ventral cord of the nematode. For the TDP-43(Q331K) transgenic model, neurodegeneration is more proximal, close to the cell bodies of GABAergic motor neurons. It would be interesting to investigate whether the pathology of TDP-43 is transferred to other neurons, like cholinergic for example, by evaluating the neurodegeneration of this neuronal subtype. Indeed, studies suggest that a proteinopathy could be transferred from a cell type to another and that this

could be a common mechanism for the onset and progression of several neurodegenerative disorders (Guo and Lee 2014, Hanspal, Dobson et al. 2017, Porta, Xu et al. 2018).

The percentage of neurodegeneration observed in endogenous mutant TDP-1(R393C) animals increased from day 1 to day 9 of adulthood, but was only significantly different from the WT control at day 9 (Fig. 5BC). This suggests that neurodegeneration appears later in this endogenous mutant comparatively to the transgenic model. Mutant TDP-1(R393C) neurodegeneration seemed to appear more on the dorsal cord of nematodes from day 1 to day 9 of adulthood (Fig. 5D). The dorsal cord corresponds to the extensions of axons starting from cell bodies of GABAergic neurons located on the ventral cord. This dorsal specificity in the endogenous mutant coincides with what is seen in patients; namely that ALS neurodegeneration begins at the distal level of axons (Moloney, de Winter et al. 2014). Like above, it would be interesting to see what happens to neurons other than GABAergic in the TDP-1(R393C) model especially because this mutant protein is expressed ubiquitously.

Effect of Edaravone and Riluzole ALS drugs

Since ALS is a complex and multifactorial disease, the development of effective therapies is a challenge for the scientific community. The only drugs approved by the FDA are Riluzole and Edaravone (Cruz 2018). Paralysis assays were performed on the transgenic mutant TDP-43(Q331K) and endogenous TDP-1(R393C) to verify whether these models respond effectively in the presence of these two ALS drugs.

The compound Riluzole, a glutamatergic neurotransmission inhibitor, did not have a neuroprotective effect in either of our models (Fig. 6AB). In some cases, it even accentuated nematode paralysis. These results were similar with another study in which Riluzole (10 µM) did not improve the paralysis rate of their mutant TDP-43(A315T) in liquid medium (Vaccaro, Patten et al. 2012). Other studies noted a modest neuroprotective effect on their *C. elegans* models, but at a higher concentration of Riluzole. Indeed, at a concentration of 33 µM, Riluzole slightly improved neuromuscular defects in a *C. elegans* model of spinal muscular atrophy (number of body bend per minute) (Dimitriadi, Kye et al. 2013). In addition, the average speed rate (mm / sec) of a pan-neuronal TDP-43 overexpression model was slightly increased when treated with 100 µM Riluzole (Ikenaka, Tsukada et al. 2019). Thus, it would be interesting to conduct additional paralysis assays to see if a higher concentration of Riluzole is required to observe a neuroprotective effect in the TDP-43(Q331K) and TDP-1(R393C) models. Another possible explanation is that the neuroprotective effect of Riluzole acts by another mechanism than the one generated by the mutant TDP-43 and TDP-1 proteins. Indeed, the biochemical target of Riluzole in motor neuron diseases is still unknown (Dimitriadi, Kye et al. 2013).

In a broader context of ALS models, one study evaluated the therapeutic effect of Riluzole on a transgenic rat model expressing human mutant protein TDP-43(M337V). Compared to the control, the administration of Riluzole (30 mg/kg/day) did not modify the various neuropathologies observed in this model (Chen, Liao et al. 2020). In addition, another study evaluated the effect of Riluzole (22 mg/kg) on three different ALS mouse models: SOD1(G93A), TDP-43(A315T) and FUS(1-359). Treatment with Riluzole had no effect on these three models' lifespan and had no significant impact on the transgenic

models FUS(1-359) and SOD1(G93A) motor performance's decline (Hogg, Halang et al. 2018). Thus, the low efficacy of Riluzole on TDP-43/TDP-1 *C. elegans* models is consistent with the effects observed in these other ALS models. Our results suggest that the excitotoxicity mechanism by which Riluzole acts might not be involved in our models. Since Riluzole was approved by the FDA in 1995 and the majority of ALS models were not yet developed, a question arises as to the standards used in the pre-clinical studies leading to the approval of this drug for ALS (Andrews, Jackson et al. 2020).

Edaravone, an antioxidant drug, possessed a neuroprotective effect on the TDP-43(Q331K) and TDP-1(R393C) models (Fig. 6CD). Indeed, the percentage of paralysis of these mutants was significantly reduced when they were treated with the compound. The percentage of paralysis of the TDP-43(WT) and WT controls remained unchanged. This suggests that maybe there is drug specificity to the type of protein involved. Very few papers have evaluated the effect of Edaravone on *C. elegans* ALS models. The exact mechanism of action of Edaravone in ALS's treatment is still unknown, but its therapeutic effect appears to be mediated by its antioxidant properties (Cruz 2018). Since Edaravone appears to be effective only for the mutant models, one possibility is that mutant TDP-43 and TDP-1 proteins are misfolded leading to ER stress (Lin, Walter et al. 2008, Vaccaro, Patten et al. 2013). Looking at other models, one study tested the effect of Edaravone on a transgenic ALS mice model expressing SOD1(G93A). Results showed that Edaravone reduced motor deficits and preserved motor neurons in the spinal cord of mice (Sawada 2017). Another group tested the effectiveness of Edaravone prior to its FDA approval on the same mutant SOD1 mouse models and showed Edaravone was effective in slowing the motor decline and motor neuron degeneration of these transgenic mice (Ito, Wate et al. 2008). Another study observed the effect of Edaravone on a transgenic SOD1(H46R) rat model and observed that treatment significantly improved motor performance of these transgenic rats (Aoki, Warita et al. 2011). Thus, Edaravone has a wide ranging neuroprotective effect on ALS mouse and rat models compared to Riluzole. The results obtained with the TDP-43/TDP-1 *C. elegans* models are consistent with these observations, suggesting a more specific activity of Edaravone to proteins associated with ALS.

Overall, our new transgenic TDP-43(Q331K) and endogenous TDP-1(R393C) *C. elegans* models recapitulate several key phenotypic aspects of ALS such as motor deficits, age-dependent neurodegeneration generating paralysis and reduced lifespan (only for the transgenic model).

The transgenic strain is the first *C. elegans* ALS model that expresses human mutant protein TDP-43(Q331K) in GABAergic motor neurons. This model displays a stronger motility phenotype, even in early adulthood. The *C. elegans* endogenous model ubiquitously expressing TDP-1(R393C) mutant protein appears to possess a more subtle motor phenotype which tends to increase in intensity over time. This mutant further reflects the genetics and pathology of ALS patients. These TDP-43 and TDP-1 models provide different physiological expression of mutant proteins and therefore phenotypes of varying intensity levels. Those range of phenotypes makes them useful tools for different approaches. For example, the TDP-43(Q331K) transgenic model would be well suited for accelerated genetic drug screening and analyzing the consequences of mutant TDP-43 protein on aggregation. As for the TDP-1(R393C) endogenous model, it would be more ideal for in-depth analysis like validation of modifiers

from other models, analyzing genetic interactions with other known ALS genes, elucidating new pathogenic mechanisms of ALS and more.

Methods And Materials

C. elegans maintenance and strains

Standard methods of culturing and handling worms were used as described previously (Stiernagle 2006). Worms were maintained on standard nematode growth media (NGM) plates that were streaked with food source OP50 *Escherichia coli* at 15°C. All experiments were conducted at 20°C. The N2 wildtype strain (WT) as well as *unc-47p::GFP* and *unc-17p::GFP;unc-47p::mCherry* were provided by the Caenorhabditis Genetics Center at the University of Minnesota. Strains *tdp-1(gk736460)* and *tdp-1(gk149996)* (TDP-1(R393C) and TDP-1(R258C)) were obtained from the Million Mutation Project (Thompson, Edgley et al. 2013). Strains *tdp-1(syb1989)* and *tdp-1(syb1905)* (crTDP-1(R393C) et crTDP-1(R258C)) were generated by CRISPR-Cas9 and obtained from SunyBiotech (Fuzhough City, Fujian, China) (Table 1). Other *C. elegans* strains used in this study can be found in Table 2. Mutant strains were outcrossed to WT at least 3 times. Homozygosity of all genotypes was confirmed by PCR or HRM. The primers used for sequencing and genotyping are listed in Table 3 and Table 4.

Table 1
Summary of models generated

Strain	Promoter	Expression	Method
TDP-43(WT) TDP-43(Q331K)	*unc-47*	GABAergic motor neurons	Transgenesis
TDP-1(R393C) TDP-1(R258C)*	*tdp-1*	Ubiquitous	Mutagenesis
TDP-1(R393C) TDP-1(R258C)*	*tdp-1*	Ubiquitous	CRISPR-Cas9
* Strains used for supplemental info.			

Table 2
Strains used

Strain name	Original strain/ cross	Name used	Genotype
PD1074	N2	WT	*Wild-type*
XQ106		unc-47 ::GFP	*unc-47p::GFP*
XQ820	XQ360	unc-47::mCherry	*unc-17p::GFP; unc-47p::mCherry*
XQ771		TDP-43(Q331K)	*unc-119(ed3); xqIs771(myo-2::mCherry; unc-47p::TDP-43(Q331K);unc-119(+))*
XQ774		TDP-43(WT)	*unc-119(ed3); xqIs774(myo-2::mCherry; unc-47p::TDP-43(WT);unc-119(+));unc-47p::GFP*
XQ777	XQ781;XQ360	TDP-1(R393C);unc-47::mCherry	*tdp-1(gk736460);unc-47p::mCherry*
XQ778*		TDP-1(R258C)	*tdp-1(gk149996)*
XQ781		TDP-1(R393C)	*tdp-1(gk736460)*
XQ795	XQ771;XQ106	TDP-43(Q331K);unc-47::GFP	*unc-119(ed3); xqIs771(myo-2::mCherry; unc-47p::TDP-43(Q331K);unc-119(+));unc-47p::GFP*
XQ797*	XQ778;XQ360	TDP-1(R258C);unc-47::mCherry	*tdp-1(gk149996);unc-47p::mCherry*
XQ841*	PHX1905	crTDP-1(R258C)	*tdp-1(syb1905)*
XQ835	PHX1989	crTDP-1(R393C)	*tdp-1(syb1989)*

* Strains used for supplemental info.

Table 3
– Primers used for sequencing

TDP-43(WT) &	Forward	5’- GTC TCT TTG TGG AGA GGA CTT GAT C -3’
TDP-43(Q331K)	Reverse	5’- GGT TTG GCT CCC TCT GCA TG -3’
TDP-1(R393C) &	Forward	5’- TGC TAC TGG TTT GAA GTA C -3’
TDP-1(R258C)	Reverse	5’- CCT CTT GTC TTA CCA ATT CT -3’
crTDP-1(R393C)	Forward	5’- AGG CTT TGC ATT CGT TAC GC -3’
	Reverse	5’- ACA CGA GTT CCG AGG TTG CC -3’
crTDP-1(R258C)	Forward	5’- CCA GTT GAC CTC ATC GTG CT -3’
	Reverse	5’- GTA ATC TTG TGG TGG GCG GA -3’

Table 4
Primers used for genotyping (PCR and HRM)

TDP-43(WT) &	Forward	5’- GTC TCT TTG TGG AGA GGA CTT GAT C -3’
TDP-43(Q331K)	Reverse	5’- GGT TTG GCT CCC TCT GCA TG -3’
TDP-1(R393C) &	Forward	5’- AAA TGA AGC ACC TCT GCC CAT G -3’
crTDP-1(R393C)	Reverse	5’- GAG AGA ATC ACC ATC CTG GT -3’
TDP-1(R258C) &	Forward	5’- TTG AGC AGA CTT TGC AGG – 3’
crTDP-1(R258C)	Reverse	5’- CTA CTT TGT CTG TGA GCC TTC C -3’

Transgenic TDP-43 nematodes and plasmid constructs

Plasmid DNA with the *tdp-43* WT or mutant gene under the control of GABA-motor neuron specific promoter (*unc- 47*) was prepared by Mutagenex using vector pCFJ212 and transgene marker *unc-119(ed3)*. The co-injection plasmid marker *myo-2::mCherry* was also used. Microinjections of plasmids and extrachromosomal array services were performed by Knudra (now called InVivo Biosystems). Plasmids were integrated using UV. Strains were outcrossed 6 times to WT. Nematodes positive for *mCherry* marker were selected and the presence of transgene was verified by PCR (Table 1).

Age-synchronized populations

To obtain an age-synchronized population of nematodes, ~4–5 adult gravid hermaphrodites were placed on 6–8 NGM plates with OP50 *E. coli* depending on the size of the desired population. Gravid hermaphrodites were allowed to lay eggs for 4-5h at room temperature before being removed from the NGM plates. Plates were kept at 20°C until the progeny reached day 1 of adulthood (~ 3 days).

Age-synchronized populations by bleaching

To obtain an age-synchronized nematode population, ~ 4–5 gravid adult hermaphrodites were placed on 8–10 NGM plates with OP50 *E. coli* depending on the size of the desired population. NGM plates were stored at 20°C until they became confluent (~ 3 days). Nematodes were collected using M9 buffer (1 M KH_2PO_4, 1 M Na_2HPO_4, 1 M NaCl and 1 M $MgSO_4$) in 15 mL Falcon tubes and were centrifuged at 4000 rpm for 4 minutes at room temperature. The supernatant was removed to leave only 7 mL of buffer in the tubes. 1 mL of 1M NaOH and 2 mL of bleach were added to reach a total volume of 10 mL. After 5 minutes of vortex, the samples were centrifuged at 4000 rpm for 4 minutes at room temperature. After removing all of the supernatant, M9 buffer was added to obtain a total volume of 10 mL. The pellet was then dissolved by vortexing and another centrifugation was performed at 4000 rpm for 4 minutes at room temperature. The steps to wash the samples were repeated two more times. After the last wash, all of the supernatant was removed. The pellet was dissolved in 1–2 mL of M9 buffer and the content was dispensed onto 8–10 NGM plates without OP50 *E. coli*. The NGM plates were stored at 20°C after allowing the M9 buffer to evaporate. After 24 hours, larvae were transferred onto NGM plates with OP50 *E. coli* using 1–2 mL of M9 buffer and then, stored at 20°C. After ~ 3 days, the nematodes reached the stage of day 1 of adulthood.

Gene expression analysis

Synchronization by bleaching was performed to obtain a population of adult day 1 nematodes. Then, the nematodes were harvest using M9 buffer in 15 mL Falcon tubes. Centrifugation at 4000 rpm for 4 minutes at room temperature was performed. All of the supernatant was removed and M9 buffer was added to obtain a total volume of 10 mL. After vortexing briefly to dissolve the pellet, another centrifugation at 4000 rpm for 4 minutes at room temperature was performed. The steps to wash the samples were repeated two more times. After the last wash, the supernatant was removed to leave only 1–2 mL. The remaining content was transferred to 2 mL Eppendorfs. Centrifugation at 4000 rpm for a few minutes at room temperature was then performed. All of the supernatant was removed, 500 µL of phenol (Trizol) were added and samples were stored at -80 ° C.

The samples were homogenized by trituration using syringes. The extraction was carried out following the protocol of the RNeasy® Lipid Tissue Mini kit by Qiagen® (Cat. No: 74804). The extracted RNA was quantified using a Nanodrop spectrophotometer and then converted into cDNA by reverse transcription. The Invitrogen ™ SuperScript ™ VILO ™ Synthesis Kit (Lot: 1756090) was used. Each well contained 4 µL of 5X VILO Reaction Mix, 2 µL of 10X SuperScript III Enzyme Blend, a predetermined volume corresponding to 663ng of RNA and RNAse-free water to complete to 20 µL. The cycle was determined according to the optimum temperature proposed by the set used (42°C).

The mRNA expression levels of the genes of interest were measured by qPCR using the Taqman Universal Master Mix II® by ThermoFisher® (Lot: 00764872). Each well contained 0.5 µL of the gene of interest probe, 5 µL of the Master Mix, 3.5 µL of H_2O and 1 µL of cDNA for a total of 10 µL. The primers used from Applied Biosystems® by Thermo Fisher Scientific® were specific for the target genes: *TARDBP* (No. Hs00606522_m1), *tdp-1* (No. Ce02436691_g1), and for the housekeeping gene *ama-1* (No. Ce02462726_m1) and *unc-47* (No. Ce02451914_g1). The device QuantStudio ™ 7 Flex Real-Time PCR System (Cat. No. 4485701) was used. All of these experiments were done in triplicate.

Lifespan assay

Following strains N2 wild-type, TDP-43(WT), TDP-43(Q331K) and TDP-1(R393C) were scored every other day from day 1 of adulthood until death. For each strain, between 30–40 adult day 1 worms (obtained via synchronization) were transferred to each of 3 NGM plates with OP50 *E. coli* and tested every other day until death. Worms were transferred to fresh plates every 2 days until the cessation of progeny production. Worms were scored as dead if they failed to respond to tactile stimulus and showed no spontaneous movement or response when prodded. Dead worms displaying whether internally hatched progeny, extruded gonads or worms that crawled off the plate were excluded. All experiments were conducted at 20°C and done in triplicates.

WormLab ®

WormLab software is an imaging, tracking and analyzing system used to analyze many parameters in a solid (crawling) or liquid (swimming) medium, such as instantaneous or average speed, wavelength, track length, body angles of flexion, average amplitude, immobility rate and more. The following strains N2 wild-type, TDP-43(WT), TDP-43(Q331K), TDP-1(R393C), crTDP-1(R393C) and TDP-1(R258C) were used to record videos of 30 seconds. For each strain, between 30–40 adult day 1 worms (obtained via synchronization) were transferred to each of 3 NGM plates without OP50 *E. coli*. For crawling parameters (speed), a 30 seconds video was taken using a CMOS camera fixed on dissecting microscope Stereomicroscope Leica S9i. For swimming parameters (speed, activity and wave initiation rate), 100 µL of M9 buffer was added on the NGM plates to submerged the worms. Then, a 30 seconds video was taken using the same camera and microscope. Worms were then transferred onto NGM plates with OP50 *E. coli* and experiment was repeated at day 5 and 9 of adulthood. Videos were analyzed using *WormLab* software and different parameters were calculated for each worm *e.g.* crawling speed, swimming speed, activity and wave initiation rate. Videos of the worms were taken on NGM plates without OP50 *E. coli* to promote locomotion and for better visualization of the nematodes by the *WormLab* software. All experiments were conducted at 20°C and done in triplicates.

Paralysis assay on solid media

Following strains N2 wild-type, TDP-43(WT), TDP-43(Q331K), TDP-1(R393C), crTDP-1(R393C), TDP-1(R258C) and crTDP-1(R258C) were scored for paralysis from day 1 to day 12 of adulthood. For each strain, between 30–40 day 1 adult worms (obtained via synchronization) were transferred to each of 3 NGM plates with OP50 *E. coli* and scored as paralysed if they failed to move after being prodded with a

worm pick without being dead. Dead worms displaying whether internally hatched progeny, extruded gonads or worms that crawled off the plate were excluded. Nematodes were transferred to fresh NGM plates every 2 days until the cessation of progeny production. All experiments were conducted at 20°C and done in triplicates.

Neuronal fluorescence microscopy

For scoring of neuronal processes for gaps or breakages in axons, following strains *unc-47p::GFP*, *unc-47p::mCherry*, TDP-43(WT);*unc-47p::GFP*, TDP-43(Q331K);*unc-47p::GFP*, TDP-1(R393C);*unc-47p::mCherry* and TDP-1(R258C);*unc-47p::mCherry* were used. Synchronized nematodes were collected at day 1, 5 and 9 of adulthood, placed on microscopy slides with 2% agarose pads and immobilized with 5 mM levamisole diluted in M9 buffer for visualization of GABAergic motoneuron processes *in vivo*. mCherry and GFP markers were visualized at 590 nm and 470 nm respectively using a Zeiss Axio Imager M2 microscope. The software used was AxioVs40 4.8.2.0. Approximately 25 worms were visualized per strain and experiment was repeated four times. The unpaired Student's t-test was applied for sets of two datasets and Bonferroni's Ordinary one-way multiple-comparison ANOVA test for sets of more than two datasets.

Compound testing on solid media

The compounds Riluzole hydrochloride (Cat. No. 0768, TOCRIS®) and Edaravone (MCI-186, Cat. No. 13320, Cayman Chemical Company) were diluted in DMSO (dimethylsulfoxide) to obtain a stock concentration of 10mM. These stock samples are stored at -20°C. The final concentration in NGM plates with OP50 *E. coli* is 20 µM for both compounds. Each compound has its negative control with the same concentration of DMSO in NGM plates with OP50 *E. coli*. Paralysis tests were performed as described previously.

Statistics

The curves of lifespan and paralysis assays were compared using the statistical log-rank test (Mantel-Cox). For the statistical analysis of the figures obtained with the WormLab® software, Ordinary one-way ANOVA with Bonferroni multiple comparison test was used. For neurodegeneration (fluorescent microscopy) and quantitative expression analysis (qPCR), the unpaired Student t test was applied for sets of two datasets and Ordinary one-way ANOVA with Bonferroni multiple comparison test for sets of more than two datasets. All the experiments were repeated at least 3 times. GraphPad Prism version 9.0.0 (86) software was used for all statistical analyzes.

Data availability

The datasets used and/or analysed during the current study available from the corresponding author on reasonable request

References

1. Abe, K., Y. Itoyama, G. Sobue, S. Tsuji, M. Aoki, M. Doyu, C. Hamada, K. Kondo, T. Yoneoka, M. Akimoto and H. Yoshino (2014). "Confirmatory double-blind, parallel-group, placebo-controlled study of efficacy and safety of edaravone (MCI-186) in amyotrophic lateral sclerosis patients." Amyotroph Lateral Scler Frontotemporal Degener **15**(7-8): 610-617.
2. Altun, Z. F. and D. H. Hall (2009). "Introduction To C. elegans Anatomy." WormAtlas.
3. Andrews, J. A., C. E. Jackson, T. D. Heiman-Patterson, P. Bettica, B. R. Brooks and E. P. Pioro (2020). "Real-world evidence of riluzole effectiveness in treating amyotrophic lateral sclerosis." Amyotroph Lateral Scler Frontotemporal Degener **21**(7-8): 509-518.
4. Aoki, M., H. Warita, H. Mizuno, N. Suzuki, S. Yuki and Y. Itoyama (2011). "Feasibility study for functional test battery of SOD transgenic rat (H46R) and evaluation of edaravone, a free radical scavenger." Brain Res **1382**: 321-325.
5. Arnold, E. S., S. C. Ling, S. C. Huelga, C. Lagier-Tourenne, M. Polymenidou, D. Ditsworth, H. B. Kordasiewicz, M. McAlonis-Downes, O. Platoshyn, P. A. Parone, S. Da Cruz, K. M. Clutario, D. Swing, L. Tessarollo, M. Marsala, C. E. Shaw, G. W. Yeo and D. W. Cleveland (2013). "ALS-linked TDP-43 mutations produce aberrant RNA splicing and adult-onset motor neuron disease without aggregation or loss of nuclear TDP-43." Proc Natl Acad Sci U S A **110**(8): E736-745.
6. Arthur, K. C., A. Calvo, T. R. Price, J. T. Geiger, A. Chiò and B. J. Traynor (2016). "Projected increase in amyotrophic lateral sclerosis from 2015 to 2040." Nat Commun **7**: 12408.
7. Balendra, R. and A. M. Isaacs (2018). "C9orf72-mediated ALS and FTD: multiple pathways to disease." Nat Rev Neurol **14**(9): 544-558.
8. Blair, I. P., K. L. Williams, S. T. Warraich, J. C. Durnall, A. D. Thoeng, J. Manavis, P. C. Blumbergs, S. Vucic, M. C. Kiernan and G. A. Nicholson (2010). "FUS mutations in amyotrophic lateral sclerosis: clinical, pathological, neurophysiological and genetic analysis." J Neurol Neurosurg Psychiatry **81**(6): 639-645.
9. Chen, S., Q. Liao, K. Lu, J. Zhou, C. Huang and F. Bi (2020). "Riluzole Exhibits No Therapeutic Efficacy on a Transgenic Rat model of Amyotrophic Lateral Sclerosis." Curr Neurovasc Res **17**(3): 275-285.
10. Cruz, M. P. (2018). "Edaravone (Radicava): A Novel Neuroprotective Agent for the Treatment of Amyotrophic Lateral Sclerosis." P t **43**(1): 25-28.
11. Dhakal, S., C. E. Wyant, H. E. George, S. E. Morgan and V. Rangachari (2020). "Prion-like C-terminal domain of TDP-43 and α-Synuclein interact synergistically to generate neurotoxic hybrid fibrils." bioRxiv: 2020.2012.2012.422524.
12. Dimitriadi, M., M. J. Kye, G. Kalloo, J. M. Yersak, M. Sahin and A. C. Hart (2013). "The neuroprotective drug riluzole acts via small conductance Ca2+-activated K+ channels to ameliorate defects in spinal muscular atrophy models." J Neurosci **33**(15): 6557-6562.
13. Flores, B. N., X. Li, A. M. Malik, J. Martinez, A. A. Beg and S. J. Barmada (2019). "An Intramolecular Salt Bridge Linking TDP43 RNA Binding, Protein Stability, and TDP43-Dependent Neurodegeneration." Cell Rep **27**(4): 1133-1150.e1138.

14. Gitler, A. D., P. Dhillon and J. Shorter (2017). "Neurodegenerative disease: models, mechanisms, and a new hope." Dis Model Mech **10**(5): 499-502.
15. Guo, J. L. and V. M. Lee (2014). "Cell-to-cell transmission of pathogenic proteins in neurodegenerative diseases." Nat Med **20**(2): 130-138.
16. Hanspal, M. A., C. M. Dobson, J. J. Yerbury and J. R. Kumita (2017). "The relevance of contact-independent cell-to-cell transfer of TDP-43 and SOD1 in amyotrophic lateral sclerosis." Biochim Biophys Acta Mol Basis Dis **1863**(11): 2762-2771.
17. Hergesheimer, R. C., A. A. Chami, D. R. de Assis, P. Vourc'h, C. R. Andres, P. Corcia, D. Lanznaster and H. Blasco (2019). "The debated toxic role of aggregated TDP-43 in amyotrophic lateral sclerosis: a resolution in sight?" Brain **142**(5): 1176-1194.
18. Hogg, M. C., L. Halang, I. Woods, K. S. Coughlan and J. H. M. Prehn (2018). "Riluzole does not improve lifespan or motor function in three ALS mouse models." Amyotroph Lateral Scler Frontotemporal Degener **19**(5-6): 438-445.
19. Ikenaka, K., Y. Tsukada, A. C. Giles, T. Arai, Y. Nakadera, S. Nakano, K. Kawai, H. Mochizuki, M. Katsuno, G. Sobue and I. Mori (2019). "A behavior-based drug screening system using a Caenorhabditis elegans model of motor neuron disease." Sci Rep **9**(1): 10104.
20. Ito, H., R. Wate, J. Zhang, S. Ohnishi, S. Kaneko, H. Ito, S. Nakano and H. Kusaka (2008). "Treatment with edaravone, initiated at symptom onset, slows motor decline and decreases SOD1 deposition in ALS mice." Exp Neurol **213**(2): 448-455.
21. Jaiswal, M. K. (2019). "Riluzole and edaravone: A tale of two amyotrophic lateral sclerosis drugs." Med Res Rev **39**(2): 733-748.
22. Johnson, T. E. and W. B. Wood (1982). "Genetic analysis of life-span in Caenorhabditis elegans." Proc Natl Acad Sci U S A **79**(21): 6603-6607.
23. Kaletta, T. and M. O. Hengartner (2006). "Finding function in novel targets: C. elegans as a model organism." Nature Reviews Drug Discovery **5**(5): 387-399.
24. Liachko, N. F., P. J. McMillan, C. R. Guthrie, T. D. Bird, J. B. Leverenz and B. C. Kraemer (2013). "CDC7 inhibition blocks pathological TDP-43 phosphorylation and neurodegeneration." Ann Neurol **74**(1): 39-52.
25. Lin, J. H., P. Walter and T. S. Yen (2008). "Endoplasmic reticulum stress in disease pathogenesis." Annu Rev Pathol **3**: 399-425.
26. Longinetti, E. and F. Fang (2019). "Epidemiology of amyotrophic lateral sclerosis: an update of recent literature." Curr Opin Neurol **32**(5): 771-776.
27. Mariol, M. C., L. Walter, S. Bellemin and K. Gieseler (2013). "A rapid protocol for integrating extrachromosomal arrays with high transmission rate into the C. elegans genome." J Vis Exp(82): e50773.
28. McIntire, S. L., R. J. Reimer, K. Schuske, R. H. Edwards and E. M. Jorgensen (1997). "Identification and characterization of the vesicular GABA transporter." Nature **389**(6653): 870-876.

29. Mejzini, R., L. L. Flynn, I. L. Pitout, S. Fletcher, S. D. Wilton and P. A. Akkari (2019). "ALS Genetics, Mechanisms, and Therapeutics: Where Are We Now?" Frontiers in Neuroscience **13**(1310).
30. Moller, A., C. S. Bauer, R. N. Cohen, C. P. Webster and K. J. De Vos (2017). "Amyotrophic lateral sclerosis-associated mutant SOD1 inhibits anterograde axonal transport of mitochondria by reducing Miro1 levels." Hum Mol Genet **26**(23): 4668-4679.
31. Moloney, E. B., F. de Winter and J. Verhaagen (2014). "ALS as a distal axonopathy: molecular mechanisms affecting neuromuscular junction stability in the presymptomatic stages of the disease." Front Neurosci **8**: 252.
32. Noma, K. and Y. Jin (2018). "Rapid Integration of Multi-copy Transgenes Using Optogenetic Mutagenesis in Caenorhabditis elegans." G3 (Bethesda) **8**(6): 2091-2097.
33. Oskarsson, B., T. F. Gendron and N. P. Staff (2018). "Amyotrophic Lateral Sclerosis: An Update for 2018." Mayo Clin Proc **93**(11): 1617-1628.
34. Pansarasa, O., M. Bordoni, L. Diamanti, D. Sproviero, S. Gagliardi and C. Cereda (2018). "SOD1 in Amyotrophic Lateral Sclerosis: "Ambivalent" Behavior Connected to the Disease." Int J Mol Sci **19**(5).
35. Patten, S. A., D. Aggad, J. Martinez, E. Tremblay, J. Petrillo, G. A. Armstrong, A. La Fontaine, C. Maios, M. Liao, S. Ciura, X. Y. Wen, V. Rafuse, J. Ichida, L. Zinman, J. P. Julien, E. Kabashi, R. Robitaille, L. Korngut, J. A. Parker and P. Drapeau (2017). "Neuroleptics as therapeutic compounds stabilizing neuromuscular transmission in amyotrophic lateral sclerosis." JCI Insight **2**(22).
36. Philip, N. S., F. Escobedo, L. L. Bahr, B. J. Berry and A. P. Wojtovich (2019). "Mos1 Element-Mediated CRISPR Integration of Transgenes in Caenorhabditis elegans." G3 (Bethesda) **9**(8): 2629-2635.
37. Pierce-Shimomura, J. T., B. L. Chen, J. J. Mun, R. Ho, R. Sarkis and S. L. McIntire (2008). "Genetic analysis of crawling and swimming locomotory patterns in C. elegans." Proc Natl Acad Sci U S A **105**(52): 20982-20987.
38. Polymenidou, M., C. Lagier-Tourenne, K. R. Hutt, C. F. Bennett, D. W. Cleveland and G. W. Yeo (2012). "Misregulated RNA processing in amyotrophic lateral sclerosis." Brain Res **1462**: 3-15.
39. Porta, S., Y. Xu, C. R. Restrepo, L. K. Kwong, B. Zhang, H. J. Brown, E. B. Lee, J. Q. Trojanowski and V. M. Lee (2018). "Patient-derived frontotemporal lobar degeneration brain extracts induce formation and spreading of TDP-43 pathology in vivo." Nat Commun **9**(1): 4220.
40. Prasad, A., V. Bharathi, V. Sivalingam, A. Girdhar and B. K. Patel (2019). "Molecular Mechanisms of TDP-43 Misfolding and Pathology in Amyotrophic Lateral Sclerosis." Front Mol Neurosci **12**: 25.
41. Rogalski, T. M. and D. L. Riddle (1988). "A Caenorhabditis elegans RNA polymerase II gene, ama-1 IV, and nearby essential genes." Genetics **118**(1): 61-74.
42. Saldi, T. K., P. E. Ash, G. Wilson, P. Gonzales, A. Garrido-Lecca, C. M. Roberts, V. Dostal, T. F. Gendron, L. D. Stein, T. Blumenthal, L. Petrucelli and C. D. Link (2014). "TDP-1, the Caenorhabditis elegans ortholog of TDP-43, limits the accumulation of double-stranded RNA." Embo j **33**(24): 2947-2966.
43. Sawada, H. (2017). "Clinical efficacy of edaravone for the treatment of amyotrophic lateral sclerosis." Expert Opin Pharmacother **18**(7): 735-738.

44. Scotter, E. L., H. J. Chen and C. E. Shaw (2015). "TDP-43 Proteinopathy and ALS: Insights into Disease Mechanisms and Therapeutic Targets." Neurotherapeutics **12**(2): 352-363.
45. Shaye, D. D. and I. Greenwald (2011). "OrthoList: a compendium of C. elegans genes with human orthologs." PLoS One **6**(5): e20085.
46. Shi, Y., S. Lin, K. A. Staats, Y. Li, W. H. Chang, S. T. Hung, E. Hendricks, G. R. Linares, Y. Wang, E. Y. Son, X. Wen, K. Kisler, B. Wilkinson, L. Menendez, T. Sugawara, P. Woolwine, M. Huang, M. J. Cowan, B. Ge, N. Koutsodendris, K. P. Sandor, J. Komberg, V. R. Vangoor, K. Senthilkumar, V. Hennes, C. Seah, A. R. Nelson, T. Y. Cheng, S. J. Lee, P. R. August, J. A. Chen, N. Wisniewski, V. Hanson-Smith, T. G. Belgard, A. Zhang, M. Coba, C. Grunseich, M. E. Ward, L. H. van den Berg, R. J. Pasterkamp, D. Trotti, B. V. Zlokovic and J. K. Ichida (2018). "Haploinsufficiency leads to neurodegeneration in C9ORF72 ALS/FTD human induced motor neurons." Nat Med **24**(3): 313-325.
47. Stiernagle, T. (2006). "Maintenance of C. elegans." WormBook: 1-11.
48. Sulston, J. E. and H. R. Horvitz (1977). "Post-embryonic cell lineages of the nematode, Caenorhabditis elegans." Dev Biol **56**(1): 110-156.
49. Tao, Q. Q. and Z. Y. Wu (2017). "Amyotrophic Lateral Sclerosis: Precise Diagnosis and Individualized Treatment." Chin Med J (Engl) **130**(19): 2269-2272.
50. Taylor, J. P., R. H. Brown, Jr. and D. W. Cleveland (2016). "Decoding ALS: from genes to mechanism." Nature **539**(7628): 197-206.
51. Thompson, O., M. Edgley, P. Strasbourger, S. Flibotte, B. Ewing, R. Adair, V. Au, I. Chaudhry, L. Fernando, H. Hutter, A. Kieffer, J. Lau, N. Lee, A. Miller, G. Raymant, B. Shen, J. Shendure, J. Taylor, E. H. Turner, L. W. Hillier, D. G. Moerman and R. H. Waterston (2013). "The million mutation project: a new approach to genetics in Caenorhabditis elegans." Genome Res **23**(10): 1749-1762.
52. Vaccaro, A., S. A. Patten, D. Aggad, C. Julien, C. Maios, E. Kabashi, P. Drapeau and J. A. Parker (2013). "Pharmacological reduction of ER stress protects against TDP-43 neuronal toxicity in vivo." Neurobiol Dis **55**: 64-75.
53. Vaccaro, A., S. A. Patten, S. Ciura, C. Maios, M. Therrien, P. Drapeau, E. Kabashi and J. A. Parker (2012). "Methylene blue protects against TDP-43 and FUS neuronal toxicity in C. elegans and D. rerio." PLoS One **7**(7): e42117.
54. Vaccaro, A., A. Tauffenberger, D. Aggad, G. Rouleau, P. Drapeau and J. A. Parker (2012). "Mutant TDP-43 and FUS Cause Age-Dependent Paralysis and Neurodegeneration in C. elegans." PLOS ONE **7**(2): e31321.
55. Vaccaro, A., A. Tauffenberger, P. E. A. Ash, Y. Carlomagno, L. Petrucelli and J. A. Parker (2012). "TDP-1/TDP-43 Regulates Stress Signaling and Age-Dependent Proteotoxicity in Caenorhabditis elegans." PLOS Genetics **8**(7): e1002806.
56. Valdmanis, P. N., H. Daoud, P. A. Dion and G. A. Rouleau (2009). "Recent advances in the genetics of amyotrophic lateral sclerosis." Current Neurology and Neuroscience Reports **9**(3): 198-205.
57. Van Deerlin, V. M., J. B. Leverenz, L. M. Bekris, T. D. Bird, W. Yuan, L. B. Elman, D. Clay, E. M. Wood, A. S. Chen-Plotkin, M. Martinez-Lage, E. Steinbart, L. McCluskey, M. Grossman, M. Neumann, I. L. Wu, W.

S. Yang, R. Kalb, D. R. Galasko, T. J. Montine, J. Q. Trojanowski, V. M. Lee, G. D. Schellenberg and C. E. Yu (2008). "TARDBP mutations in amyotrophic lateral sclerosis with TDP-43 neuropathology: a genetic and histopathological analysis." Lancet Neurol **7**(5): 409-416.

58. White, M. A., E. Kim, A. Duffy, R. Adalbert, B. U. Phillips, O. M. Peters, J. Stephenson, S. Yang, F. Massenzio, Z. Lin, S. Andrews, A. Segonds-Pichon, J. Metterville, L. M. Saksida, R. Mead, R. R. Ribchester, Y. Barhomi, T. Serre, M. P. Coleman, J. R. Fallon, T. J. Bussey, R. H. Brown, Jr. and J. Sreedharan (2018). "TDP-43 gains function due to perturbed autoregulation in a Tardbp knock-in mouse model of ALS-FTD." Nat Neurosci **21**(4): 552-563.
59. Wong, S. Q., M. G. Pontifex, M. M. Phelan, C. Pidathala, B. C. Kraemer, J. W. Barclay, N. G. Berry, P. M. O'Neill, R. D. Burgoyne and A. Morgan (2018). "α-Methyl-α-phenylsuccinimide ameliorates neurodegeneration in a C. elegans model of TDP-43 proteinopathy." Neurobiol Dis **118**: 40-54.
60. Zarei, S., K. Carr, L. Reiley, K. Diaz, O. Guerra, P. F. Altamirano, W. Pagani, D. Lodin, G. Orozco and A. Chinea (2015). "A comprehensive review of amyotrophic lateral sclerosis." Surgical neurology international **6**: 171-171.
61. Zhang, T., H. Y. Hwang, H. Hao, C. Talbot, Jr. and J. Wang (2012). "Caenorhabditis elegans RNA-processing protein TDP-1 regulates protein homeostasis and life span." J Biol Chem **287**(11): 8371-8382.

Figures

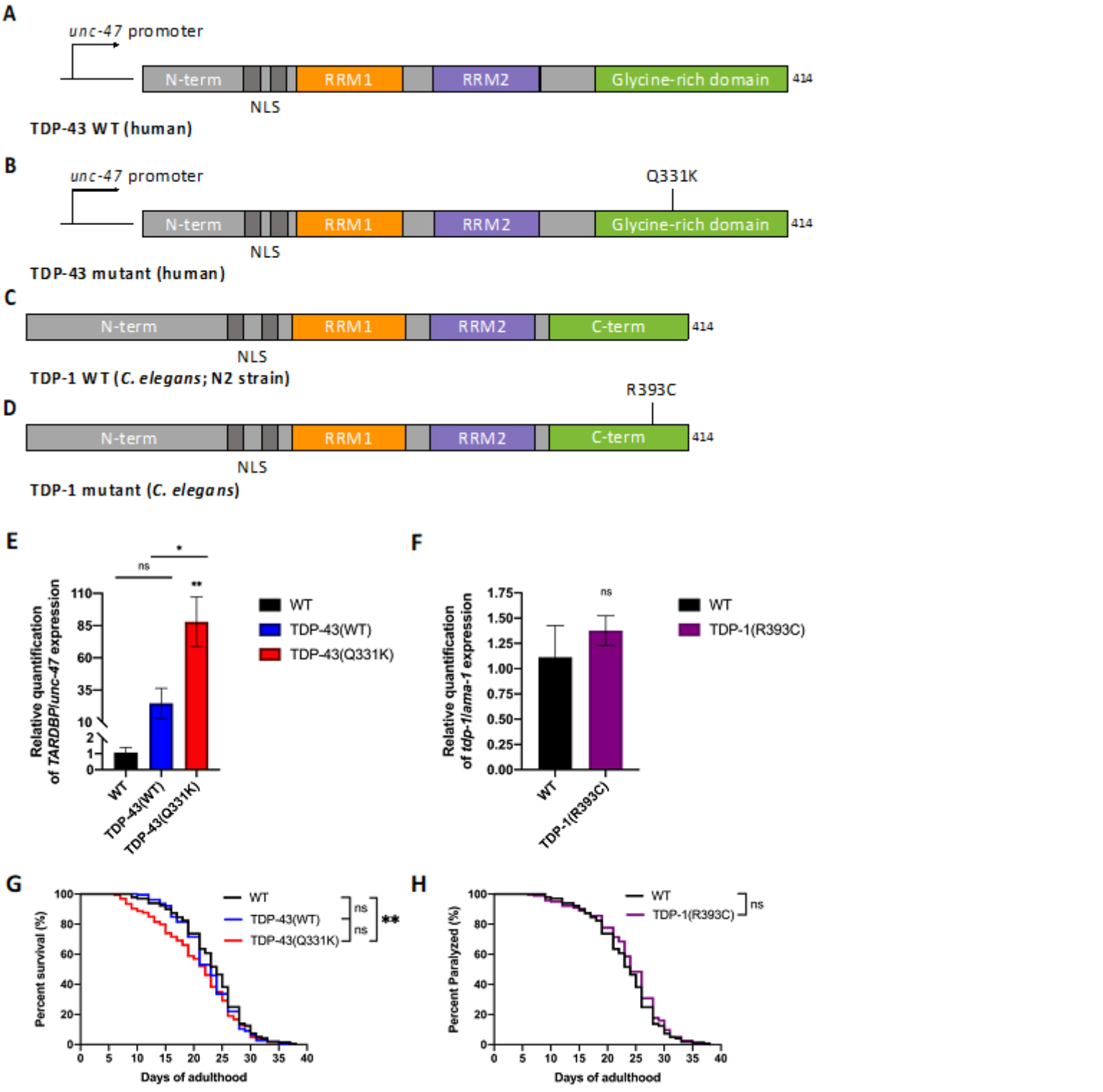

Figure 1

Wild-type/mutant TDP-43 transgenic and TDP-1 endogenous models with their *TARDBP* and *tdp-1* mRNA relative quantification expression levels have little or no effect on lifespan.

(A) Full-length wild-type human TDP-43 (isoform 1) or (B) full-length mutant human TDP-43 containing *Q331K* mutation were obtained by transgenesis and expressed under *unc-47* promoter. N-term, N-terminal

region; NLS, nuclear localization signal; RRM1, RNA recognition motif 1; RRM2, RNA recognition motif 2; Glycine-rich domain, C-terminal region composed of a glycine-rich domain. (C) Full-length wild-type *C. elegans* TDP-1 protein found in N2 strain (isoform c). (D) Full-length mutant *C. elegans* TDP-1 containing *R393C* mutation (isoform c) was obtained by mutagenesis or CRISPR-Cas9. N-term, N-terminal region; NLS, nuclear localization signal; RRM1, RNA recognition motif 1; RRM2, RNA recognition motif 2; C-term, C-terminal region without a glycine-rich domain. (E) Relative quantification by RT-qPCR of *TARDBP* mRNA expression levels normalized by the endogenous *unc-47* gene (codes for a transmembrane vesicular GABA transporter in GABAergic neurons in *C. elegans*) (McIntire, Reimer et al. 1997) for the TDP-43 transgenic models [**P*<0.05, ***P*<0.01, by Ordinary one-way ANOVA Bonferroni's multiple comparisons test]. (F) Relative quantification by RT-qPCR of *tdp-1* mRNA expression levels normalized by the endogenous *ama-1* gene (RNA polymerase II subunit in *C. elegans*) (Rogalski and Riddle 1988) for the endogenous TDP-1 model [ns: not significant, by the unpaired Student t test]. (G) Percent survival (%) of nematodes according to days of adulthood. TDP-43(Q331K) has reduced lifespan compared with WT but not with TDP-43(WT) [***P*<0.01, by log-rank (Mantel-Cox) test; *n*=240-280]. (H) TDP-1 mutation did not have an effect on lifespan [ns: non-significant, by log-rank (Mantel-Cox) test; *n*=280-315]. These experiments were repeated three times.

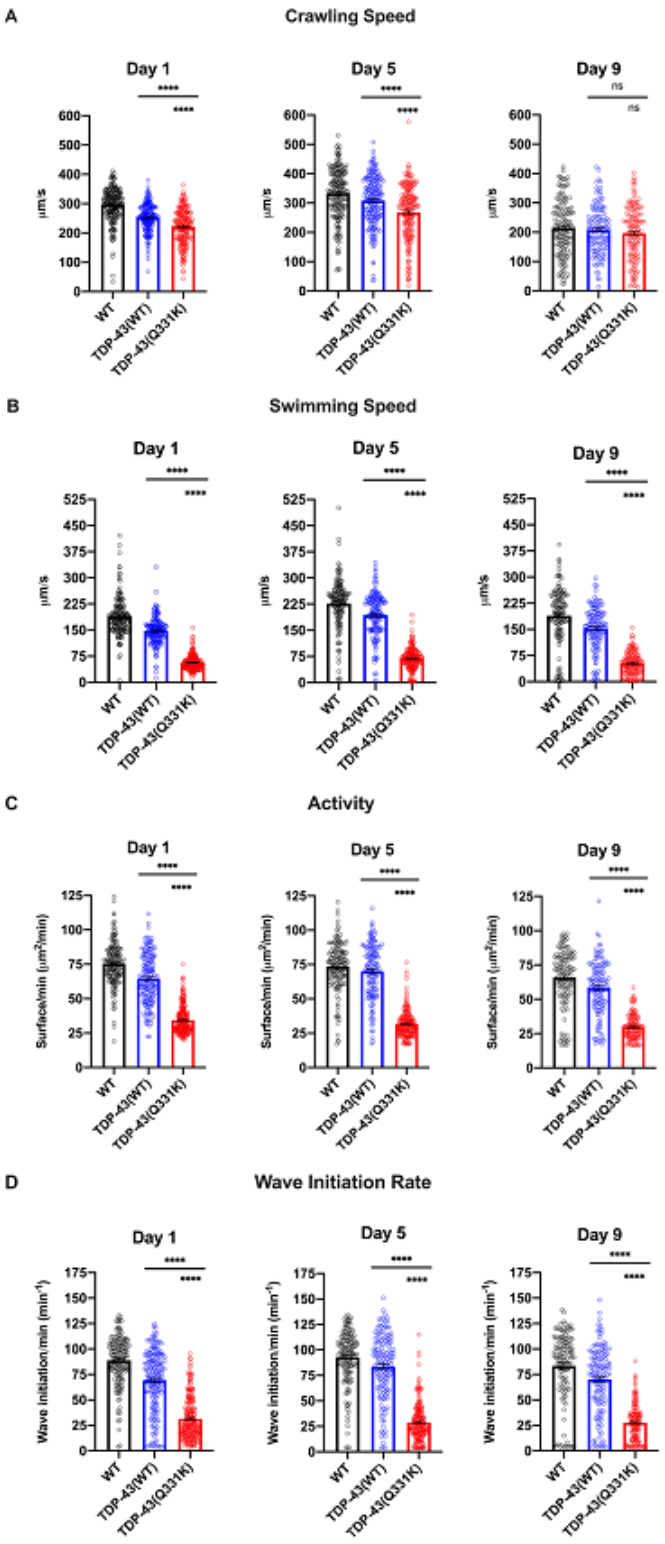

Figure 2

TDP-43 transgenic mutant exhibits a motility phenotype during aging.

(A) Nematode crawling speed (µm/s) at day 1, 5 and 9 of adulthood. TDP-43(Q331K) has a significantly lower crawling speed compared with TDP-43(WT) or WT at day 1 and 5 of adulthood [****P<0.0001, by Ordinary one-way ANOVA Bonferroni's multiple comparisons test; n=123-220]. All crawling speeds seem

to stabilize by day 9 of adulthood. (B) Nematode swimming speed (μm/s) at day 1, 5 and 9 of adulthood. TDP-43(Q331K) has a significantly lower swimming speed compared with TDP-43(WT) or WT at day 1, 5 and 9 of adulthood [****P<0.0001, by Ordinary one-way ANOVA Bonferroni's multiple comparisons test; n=129-239]. (C) Nematode swimming activity (surface/min) at day 1, 5 and 9 of adulthood. It represents the surface covered (μm^2) by the animals during one minute of swimming. TDP-43(Q331K) swimming activity is significantly lower compared to TDP-43(WT) or WT at day 1, 5 and 9 of adulthood [****P<0.0001, by Ordinary one-way ANOVA Bonferroni's multiple comparisons test; n=129-239]. (D) Wave initiation rate of nematodes at day 1, 5 and 9 od adulthood. Wave initiation rate is the number of body waves initiated by the head or the tail per minute of swimming. TDP-43(Q331K) wave initiation rate is significantly lower compared to TDP-43(WT) or WT at day 1, 5 and 9 of adulthood. [****P<0.0001, by Ordinary one-way ANOVA Bonferroni's multiple comparisons test; n=129-239]. Experiments were repeated three times.

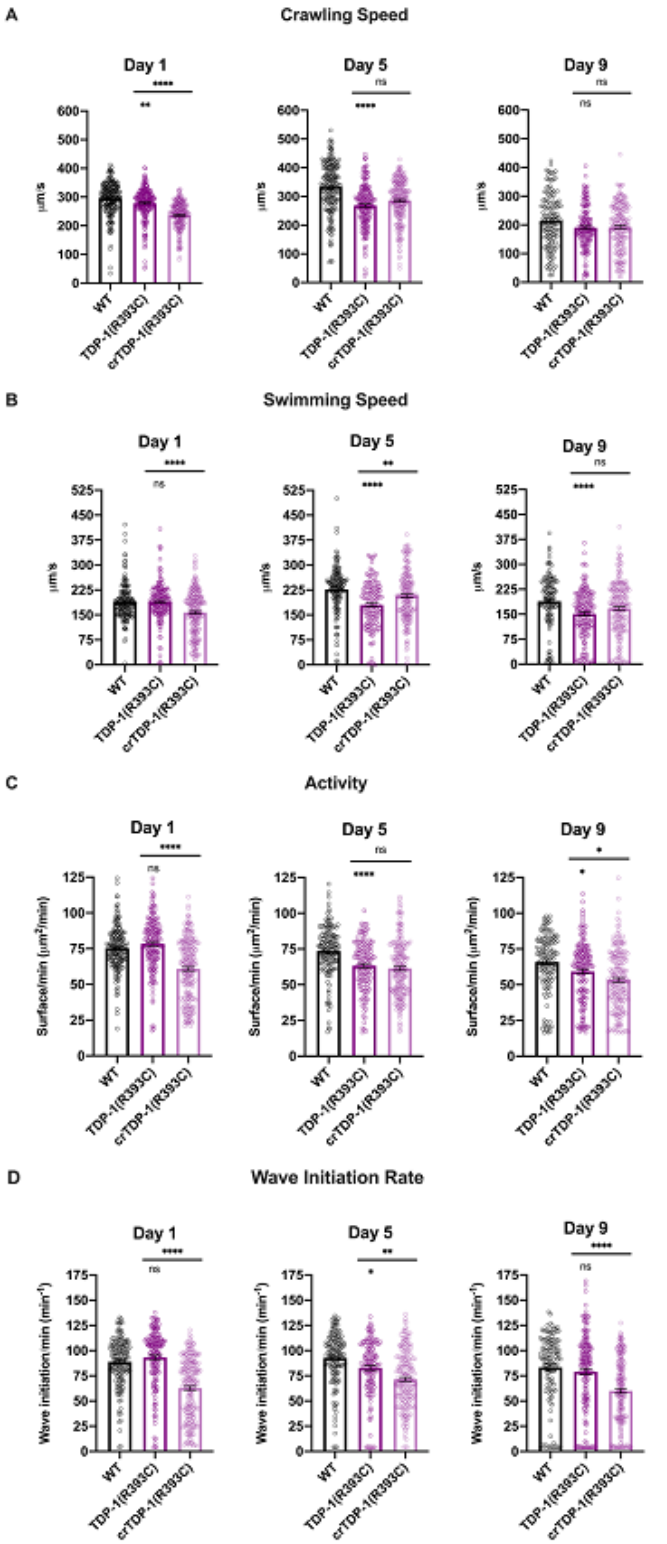

Figure 3

TDP-1 endogenous mutant exhibits a motility phenotype during aging.

(A) Nematode crawling speed (µm/s) at day 1, 5 and 9 of adulthood. TDP-1(R393C) has a decreased crawling speed than WT at day 1 of adulthood and it decreases even more at day 5. All crawling speeds seem to stabilize by day 9 of adulthood. The crawling speed of the positive control crTDP-1(R393C) is

similar to the mutant TDP-1(R393C) at day 5 and 9 of adulthood only [**P<0.005,****P<0.0001, by Ordinary one-way ANOVA Bonferroni's multiple comparisons test; n=140-230]. (B) Nematode swimming speed (μm/s) at day 1, 5 and 9 of adulthood. TDP-1(R393C) has no significantly different swimming speed compared to WT at day 1 of adulthood but it significantly decreased at day 5 and 9 of adulthood compared to WT. The swimming of the positive control crTDP-1(R393C) is similar to mutant TDP-1(R393C) except at day 1 [**P<0.005, ****P<0.0001, by Ordinary one-way ANOVA Bonferroni's multiple comparisons test; n=129-226]. (C) Nematode swimming activity (surface/min) at day 1, 5 and 9 of adulthood. It represents the surface covered (μm^2) by the animals during one minute of swimming. TDP-1(R393C) swimming activity is not significantly different than WT at day 1 of adulthood but it gradually decreases at day 5 and 9. The activity of the positive control crTDP-1(R393C) is similar to the mutant TDP-1(R393C) except at day 1 of adulthood [*P<0.05, ****P<0.0001, by Ordinary one-way ANOVA Bonferroni's multiple comparisons test; n=129-226]. (D) Wave initiation rate of nematodes at day 1, 5 and 9 of adulthood. Wave initiation rate is the number of body waves initiated by the head or the tail per minute of swimming. The wave initiation rate of mutant TDP-1(R393C) is not significantly different than WT at day 1 of adulthood. The wave initiation rate significantly decreases at day 5 of adulthood compared to WT but becomes non-significant again at day 9. The wave initiation rate of the positive control crTDP-1(R393C) is significantly different from mutant TDP-1(R393C) [*P<0.05, **P<0.001, ****P<0.0001, by Ordinary one-way ANOVA Bonferroni's multiple comparisons test; n=129-226]. Experiments were repeated three times.

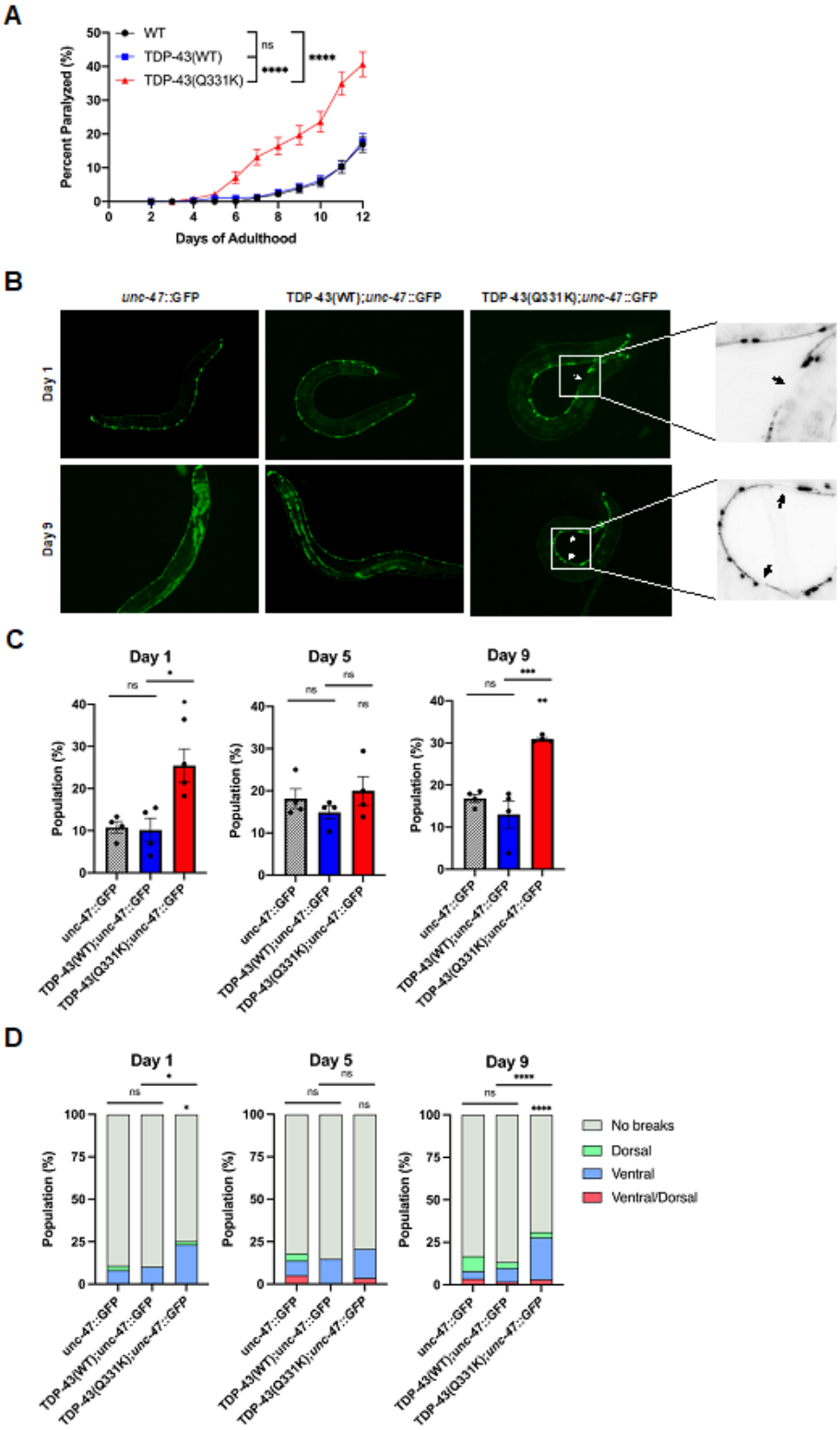

Figure 4

Transgenic mutant TDP-43 exhibits a motor defect phenotype and more ventral age-dependent neurodegeneration.

(A) Percent paralyzed (%) of nematodes according to days of adulthood. TDP-43(Q331K) has a significantly higher paralysis phenotype than TDP-43(WT) and WT [****P<0.0001, by log-rank (Mantel-

Cox) test; *n*=248-315]. The experiment was repeated three times. (B) Mosaic of fluorescence microscopy images at day 1 and 9 of adulthood according to the *unc-47::GFP* reporter in GABAergic motor neurons. Arrows indicate breaks on axonal projections of the ventral cord. (C) Percentage of nematode population with neurodegeneration at day 1, 5 and 9 of adulthood. Each dot represents the average percentage of neurodegeneration of approximately 25 worms. Mutant TDP-43(Q331K) has a significantly higher percentage of neurodegeneration than the *unc-47::GFP* and TDP-43(WT) controls at day 1 and 9 of adulthood [**P*<0.05, ***P*<0.005, ****P*<0.0005, by Ordinary one-way ANOVA Bonferroni's multiple comparisons test; n=97-116]. (D) Counting of neurodegeneration at day 1, 5 and 9 of adulthood depending on whether breaks are found on the ventral or the dorsal cord of nematodes. Transgenic strains TDP-43(WT) and TDP-43(Q331K) showed more breaks on the ventral cord of axonal projections [comparing the ventral category: **P*<0.05, *****P*<0.0001, by Ordinary one-way ANOVA Bonferroni's multiple comparisons test; n=97-116]. The experiment was repeated four times.

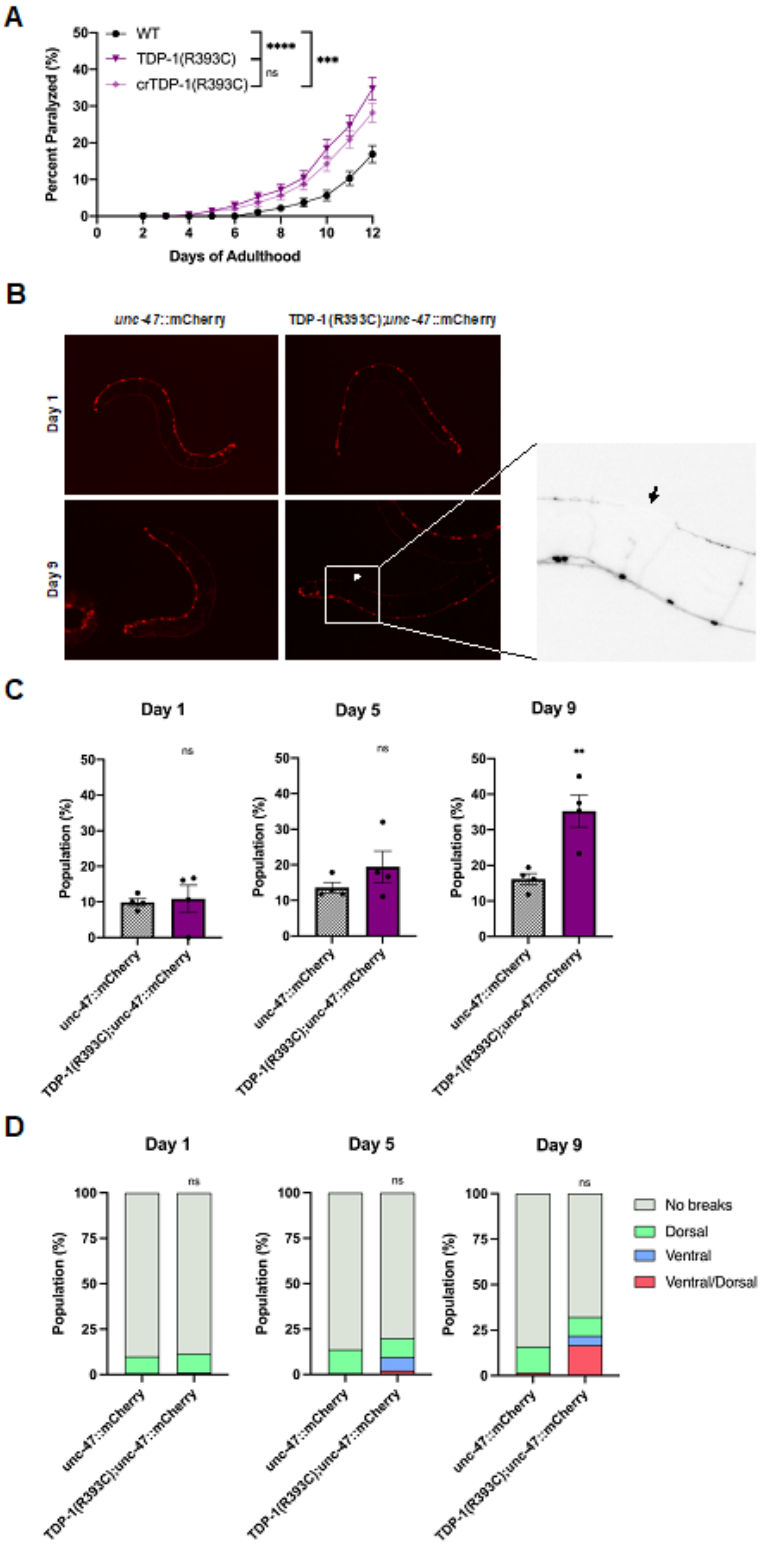

Figure 5

Endogenous mutant TDP-1 exhibits a motor defect phenotype and more dorsal age-dependent neurodegeneration.

(A) Percent paralyzed (%) of nematodes according to days of adulthood. TDP-1(R393C) has a less severe motility phenotype but still significantly different from WT. Positive control crTDP-1(R39C) has a

paralysis phenotype similar to the endogenous mutant [***P<0.001, ****P<0.0001, by log-rank (Mantel-Cox) test; n=248-314]. The experiment was repeated three times. (B) Mosaic of fluorescence microscopy images at day 1 and 9 of adulthood according to the *unc-47::mCherry* reporter in GABAergic motor neurons. Arrows indicate breaks on axonal projections of the dorsal cord. (C) Percentage of nematode population with neurodegeneration at day 1, 5 and 9 of adulthood. Each dot represents the average percentage of neurodegeneration of approximately 25 worms. Mutant TDP-1(R393C) has a significantly higher percentage of neurodegeneration than the *unc-47::mCherry* control at day 9 of adulthood [**P<0.01, by the unpaired Student t test; n=95-138]. (D) Counting of neurodegeneration at day 1, 5 and 9 of adulthood depending on whether the fluorescence breaks are found on the ventral or the dorsal cord of nematodes. Endogenous mutant TDP-1(R393C) showed more breaks on the dorsal cord of axonal projections [comparing the dorsal category: ns: non-significant P>0.1, by the unpaired Student t test; n=95-138]. The experiment was repeated four times.

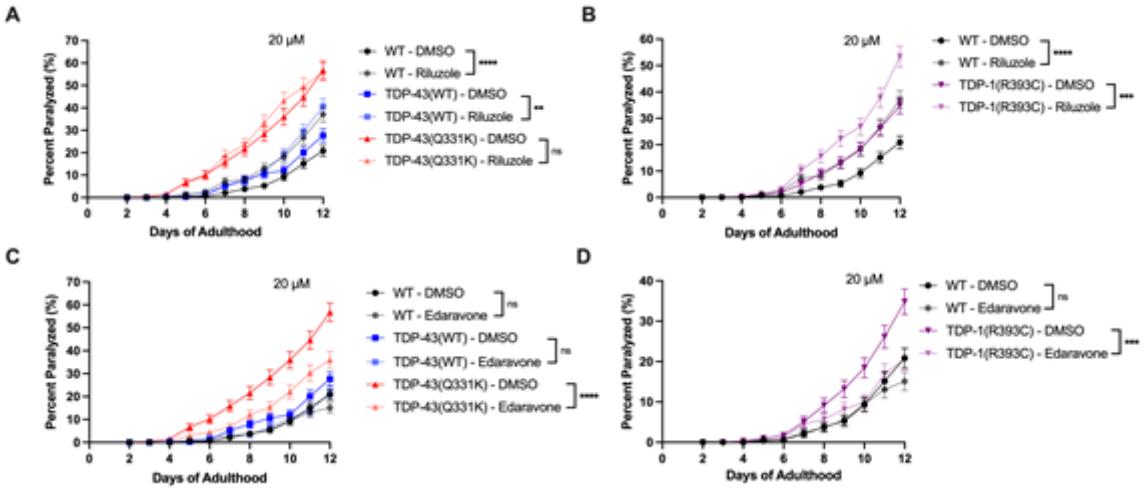

Figure 6

Neuroprotective effect of ALS drugs, Riluzole and Edaravone, on transgenic TDP-43(Q331K) and endogenous TDP-1(R393C) mutants

Percentage (%) of paralyzed nematodes according to days of adulthood. (A) Mutant TDP-43(Q331K) treated with 20 µM of Riluzole does not have a paralysis rate significantly different from the untreated transgenic mutant (20 µM of DMSO). WT and TDP-43(WT) controls treated with 20 µM of Riluzole show a significantly higher paralysis rate than untreated controls [ns: non-significant P>0.5, **P<0.01, ****P<0.0001, by log-rank (Mantel-Cox) test; n=270-325]. (B) TDP-1(R393C) and WT strains treated with 20 µM of Riluzole have a significantly higher paralysis rate than those untreated (20 µM of DMSO) [***P<0.0005, ****P<0.0005, by log-rank (Mantel-Cox) test; n=307-325]. (C) Mutant TDP-43(Q331K) treated with 20 µM of Edaravone has a significantly reduced paralysis rate compared to the untreated transgenic mutant (20 µM of DMSO). WT and TDP-43(WT) controls treated with 20 µM of Edaravone do not have a significantly different paralysis rate from the untreated controls [ns: non-significant P>0.1,

****P<0.0001, by log-rank (Mantel-Cox test); n=270-325]. (D) Mutant TDP-1(R393C) treated with 20 μM of Edaravone shows a significantly lower paralysis rate than the untreated endogenous mutant (20 μM of DMSO). WT control treated with 20 μM of Edaravone does not have a significantly different paralysis rate compared with the untreated WT control [ns: non-significant P>0.1, ***P<0.001, by log-rank (Mantel-Cox) test; n=315-325]. The experiment was repeated three times.

Supplementary Files

This is a list of supplementary files associated with this preprint. Click to download.

- SupplementaryMaterialSection.docx